Dios, M.; Gonzalez, Z.; Gordo, E.; Ferrari, B. (2016). Chemical precipitation of nickel nanoparticles on TI(C,N) suspensions focused on cermet processing. *International Journal of Refractory Metals and Hard Materials*.
DOI: 10.1016/j.ijrmhm.2016.08.009

Chemical precipitation of nickel nanoparticles on Ti(C,N) suspensions focused on cermet processing

M. Dios [a,*], Z. Gonzalez [b,c], E. Gordo [a], B. Ferrari [b]

[a] Department of Materials Science and Engineering and Chemical Engineering, University Carlos III of Madrid, Avda. Universidad 30, 28911 Leganés, Madrid, Spain
[b] Institute of Ceramic and Glass, CSIC, C/Kelsen 5, 28049 Madrid, Spain
[c] Hispano Italiana de Revestimientos S.A, Santander, Spain

A B S T R A C T

Ti(C,N) based cermets are currently used in high speed cutting tools industry due to its high thermal stability. In previous works, Fe was proposed as metal matrix, however the use of iron as continuous matrix strongly affects the processing due to the low wetting capability of molten Fe with the reinforcement phase, Ti(C,N). To solve this problem, the use of alloys such as FeNi has been proposed, where Ni improves the wettability between the ce ramic and the metal phases. This work proposes a bottom up approach to build the cermet microstructure through the synthesis of metal nanoparticles (NPs) on the surface of Ti(C,N) micrometric particles, creating Ti(C,N) Ni core shell structures. For that purpose, the in situ synthesis of Ni NPs through the chemical reduction of a Ni precursor onto the surface of micrometric Ti(C,N) particles, previously stabilized in an aqueous suspen sion, was proposed. Core shell structures were characterized by X Ray Diffraction (XRD), scanning electron mi croscopy (SEM), field emission scanning electron microscopy (FE SEM), scanning transmission electron microscopy (STEM), high resolution scanning electron microscopy (HRTEM), energy dispersive X Ray spectros copy (EDX) and Raman Spectroscopy.

1. Introduction

Compared to cemented carbides, titanium carbonitride (Ti(C,N)) based cermets are gaining increasing technical importance, due to their excellent and unique combination of physical properties such as high melting point, hardness, thermal conductivity, wear resistance and good chemical and thermal stability [1]. In the production of Ti(C,N) based cermets, the starting materials are typically Ti(C,N) and a metal binder that is usually Ni, Co, or a combination of both. Tradition ally, in order to obtain a well controlled microstructure, cermets are produced by ball milling during long time or mechano chemical routes, leading to risks of contamination with the milling media [2,3]. However, the reduction in both, content and size of the binder phase, can be also achieved by bottom up approaches, mainly profiting from the chemical routes such as electroless processes [4,5]. In this sense, the electroless Ni plating has been widely used to modify the surface of many substrates, whatever was their electrical nature (nonconductors, semiconductors and metals). This plating method is scalable, inexpensive and leads to a high and uniform coating yield, and recently it has been also used to coat and decorate micro and NPs [6 8].

Metal coated ceramic powders refer to composite powders with a ceramic core and a metal shell that can endow the ceramic particles with particular electrical, magnetic and chemical properties [9], and si multaneously improve surface properties such as wetting or joining. Re cently, core shell structures have been fabricated successfully in a number of materials with various methods, including self assembly, sonochemistry, vapor deposition polymerization or chemical vapor liquid reaction. In this sense, the present work is aimed to develop an al ternative route of fabrication of Ti(C,N) based cermets by the electroless chemical reduction of a precursor to produce Ni NPs onto the surface of micrometric Ti(C,N) particles, producing core shell composites as starting material for further processing.

The Ni precipitation in an alkaline bath is a common method to ob tain NPs by homogeneous synthesis. Among other reducing agents, hy drazine is one of the most regularly used. Hydrazine has a standard reduction potential of −1.16 V (Eq. (1)) in an alkaline solution, while Ni has a standard reduction potential of −0.25 V, and consequently it can be easily reduced by hydrazine (Eq. (2)). Therefore, the chemical re duction process of the Ni^{2+} ions can be simply shown in the Eq. (3), were the solution pH noticeably influences the synthesis of the Ni NPs.

$$N_2H_4 + 4OH \quad N_2 + 4H_2O + 4e \;; E_0 \quad -1.16\ V \tag{1}$$

$$2Ni^{2+} + 4e \quad 2Ni; E_0 \quad -0.25\ V \tag{2}$$

* Corresponding author.
E-mail address: midiosp@ing.uc3m.es (M. Dios).

$$2Ni^{2+} + N_2H_4 + 4OH \leftrightarrow 2Ni + N_2 + 4H_2O \quad (3)$$

Many formulations of the precursor solution and protocols have been described in the literature for the homogeneous synthesis of Ni NPs. Table 1 summarizes main synthesis conditions, such as solvent, Ni precursor, reducing agent, activation procedure as well as the resulting size and morphology of Ni particles. In 2003, S.H. Wu et al. [10] described the synthesis of Ni NPs 9.2 nm in diameter. They used hydrazine for the reduction of nickel chloride in ethylene glycol at 60 °C, and suggest the role of the own solvent to prevent particle agglomeration. One year later, K.H. Kim et al. [11], reported a similar synthesis route using alcohols as solvents and carboximetilcellulose (Na CMC) as processing additive, proving the effect of the variation of the reaction temperature, the length of solvent chain, and Ni^{2+} concentration [12]. They demonstrate that NPs size increases from approximately 150 nm up to 1 μm, with the temperature, the number of carbons of the solvents and the precursor concentration, being the Ni content the more drastic parameter. Contrarily, the addition of Na CMC prevented agglomeration, and contributed to the synthesis of NPs. Finally, results in those works evidenced a lack of crystallinity of the produced Ni due to the fast reduction process when using hydrazine. Chen Rui Ying et al. [13] studied the effects of reaction temperature and flow rate of a nickel sulfate solution in a flow reactor, obtaining Ni NPs of 100 nm with a narrow size distribution, while J.W. Park et al. [14] suggested a two steps synthesis process in deionized (DI) water, that includes the formation of nickel hydroxide and its further reduction by a ligand exchange reaction between a nickel hydrazine complex and the base, NaOH. The standard deviation of the size of NPs decreased with the concentration of nickel hydrazine complex while the mean particle size increased.

More recently, G.G. Couto et al. [15] reported the synthesis of Ni NPs ranging 3.4 7.7 nm in diameter, using poly N vinilpyrrolidone (PVP) as protective agent, sodium borohydride as reducing agent, nickel chloride as precursor and a mixture of ethylene glycol, acetone and ethanol as solvent. The presence of PVP was considered essential to prevent the aggregation and addressed the NPs growing. D.P. Wang et al. [16] using the same solvent and CTAB as size modifier and nickel sulfate as precursor, were able to synthesized Ni spheres of 30 nm in diameter. They identified the effect of the use of water as solvent and the surfactant addition on the morphology of the products. Finally, they describe the synthesis of flowerlike powders for high concentrations of Ni^{2+}, shaped by the aggregation of spherical NPs, but also platelet shaped particles (80 to 120 nm in diameter), due to the polarity of water molecules. Special conditions of synthesis, as the application of inert gas and ultrasounds during the reduction reaction, were tested by Z.G. Wu et al. [17] and J. Tientong et al. [18], respectively, obtaining pure Ni at room temperature without any organic additive, using as solvents an alcoholic mixture and water respectively. Those authors demonstrate that to get well dispersed Ni powder without particle agglomeration, a proper Ni^{2+} concentration is needed, and a pH value over 9.5 in the precursor bath.

Considering the procedures described in the literature in a previous work [19], the homogeneous chemical reduction of a Ni^{2+} salt in aqueous solution with hydrazine was studied. In order to obtain Ni NPs, ultrasounds will be used as activation force to disperse Ni nuclei and promote the precipitation, avoiding the chemical activation of regular electroless methods to suppress further cleaning and drying steps during the processing. The influence of variables such as Ni^{2+} concentration, reducing agent ratio, temperature, time and US power, were evaluated. The most advantageous conditions according to the needs and desired properties of the obtained Ni NPs, were selected to optimize the coverage of Ti(C,N) particles. Consequently a bottom up route for obtaining Ti(C,N)/Ni core shell particles is proposed. Unlike what it has been commonly found in literature, this route consists in the electroless chemical reduction of a nickel salt to metallic Ni NPs in aqueous solution, avoiding the use of any other kind of solvent resulting in an environmentally friendly route. Ni nitrate was used as Ni precursor instead of the more common use of chlorides, sulfates and acetates, harmful precursors to the metal matrix.

2. Experimental procedure

As received Ti(C,N) powder with a mean particle size of 2.1 μm (Grade C, H.C. Starck GmbH, Germany) were used as ceramic phase. The Ni precursor was nickel nitrate hexahydrate ($Ni(NO_3)_2 \cdot 6H_2O$, Panreac, Spain); Potassium hydroxide (KOH, Panreac, Spain) and hydrazine monohydrate ($N_2H_4 \cdot H_2O$, Sigma Aldrich, Germany) were used as a base and reducing agent, respectively. All chemicals had analytical grade and were used without any further purification. DI water was also used as solvent to prepare the mixture of KOH/N_2H_4.

Ti(C,N) suspensions with a 3 vol.% solid content were prepared using DI water as described elsewhere [20]. The procedure to synthesize the Ni nanoparticles was similar to that used for the homogeneous precipitation described elsewhere [19]. The Ni precursor, was dissolved in the suspension vehicle (DI water) before the Ti(C,N) particles addition, and then, the suspension was maintained at its natural pH (pH 7 8). The precipitation of Ni NPs was activated by the addition of a mixture of hydrazine and potassium hydroxide during the application of ultrasounds (US), using a US probe of 200 W (Sonopuls HD 2200, Bandelin electronic, Germany).

The Ni^{2+} concentration was fixed as reference to 0.1 M for coating Ti(C,N) particles. The molar ratios among reactants were 1 Ni^{2+}: 10 KOH: X $N_2H_4 \cdot H_2O$, being X = 30 and 60 (labelled Ni30Hz and Ni60Hz, respectively). Core shell structures were obtained by the chemical precipitation of Ni NPs onto the surface of micrometric Ti(C,N) particles. These particles, previously stabilized in the aqueous

Table 1
Summary of main parameters of the syntheses and the characteristics of Ni NPs.

Nickel precursor	Synthesis solvent	Reductor	Additive	Process and time	T (°C)	Particle size	Ref
Nickel chloride	Ethylene glycol	Hydrazine	–	Heating and stirring for 60 min	60 °C	9.2 nm	[10]
Nickel chloride	Ethanol 1-Propanol 1-Butanol	Hydrazine	Na-CMC	Heating and stirring for 45 min	40 °C–80 °C	160 nm to 650 nm	[11]
Nickel chloride	1-Propanol	Hydrazine	Na-CMC	Heating and stirring for 45 min	60 °C	500 nm to 1.9 μm	[12]
Nickel sulfate	Ethanol	Hydrazine	–	Heating and stirring	53 °C–73 °C	100 nm to 700 nm	[13]
Nickel chloride	DI water	Hydrazine	–	Heating and stirring for 60–120 min	60 °C	150 nm–380 nm	[14]
Nickel chloride	Ethylene glycol Acetone Ethanol	Sodium borohydride	PVP	Heating and stirring for 120 min	140 °C	3.4 nm–3.8 nm	[15]
Nickel sulfate	Ethylene glycol acetone Ethanol	Hydrazine	CTAB	Heating and stirring for 50 min Heating and resting for 60 min	75 °C	30 nm–400 nm	[16]
Nickel chloride	Alcohol Acetone	Hydrazine	–	Heating and stirring for 120 min	Room	50 nm	[17]
Nickel chloride	DI water	Hydrazine	PVP	Sonication for 30 min	60 °C	7–14 nm	[18]

solution, were used as seeds. Ni NPs precipitate under US application when the KOH/N_2H_4 mixture was poured into the Ti(C,N) suspen sion. US were applied with a 100% of the nominal probe power, dur ing 5 min, maintaining the temperature of the suspension below 50 °C, by external refrigeration with a cryothermal bath. US achieves 2.16 W/mol·s considering the fitted Ni^{2+} concentration.

The formulation of the Ti(C,N) suspension and Ni^{2+} solution, was done for a final composition of Ti(C,N) Ni composites (core shell parti cles) of 96/4 v/v Ti(C,N)/Ni (labelled 4Ni**30**Hz and 4Ni**60**Hz depending on the amount of hydrazine). To determine the composition of the core shell structures, the powder obtained after the synthesis was dried at room conditions and analyzed by X ray diffraction (XRD, Siemens Bruker D8 Advance Diffractometer, Germany) using Cu Kα ra diation (λ = 1.540598 Angstrom). The diffraction patterns were mainly measured step by step (0.05° and 0.02° in 2Θ).

In order to determine the growth mechanism of the Ni NPs onto the Ti(C,N) particles, a Ni60Hz synthesis was done varying one order of magnitude the concentration of Ni^{+2} (from 0.1 to 0.01 M) and varying the volumetric ratio Ti(C,N)/Ni from 96/4 v/v to 90/10 v/v (labelled **4**Ni60Hz and **10**Ni60Hz depending on the amount of Ni expected at the final composite). Composites produced from those syntheses were studied by field emission scanning electron microscopy (FE SEM, S 4700 microscope, Hitachi, JAPAN), high resolution transmission elec tron microscopy (HR TEM, JEOL JEM 2011 (Jeol Ltd., Japan), scanning transmission electron microscopy (STEM), selected area electron dif fraction (SAED) and EDX. Table 2 summarizes the formulation of the syntheses and the expected composition of the produced composites.

Tailored powders were directly shaped by slip casting in a po rous mold made on plaster of Paris. Green samples were sintered at 1450 °C for 60 min in vacuum (10^{-5} atm) [21]. The micrographs of the obtained bulk pieces were recorder using scanning electron microscopy (SEM, Philips XL 30, Hitachi, JAPAN) and the final com position was analyzed by Energy dispersive X ray spectroscopy (EDX, Philips DX4, Hitachi, Japan).

Raman spectroscopy was used to approach the composite crystallog raphy using a micro Raman system with a 532 nm excitation laser a 50× objective. The incident laser power was 10 mW and the optical res olution diffraction of the Confocal microscope was limited to 200 nm laterally and 500 nm vertically. Collected spectra were analyzed with the Witec Control Plus Software (Witec, Ulm, Germany).

3. Results and discussion

Fig. 1a shows the XRD pattern of the as received Ti(C,N) particles and Fig. 1b the XRD pattern corresponding to Ni NPs obtained from a homo geneous synthesis performed under selected conditions [22]. XRD pat tern of as received ceramic corresponds to the main reflections of Ti(C,N) (indexed using JCPDS card 042 1488), while as synthesized Ni pattern (Fig. 1b) shows the three characteristic peaks of the FCC lattice of Ni (45°, 52.4°, 76.9°), corresponding to Miller indices (111), (200) and (222) (indexed using JCPDS card 04 0850). Crystallite size of Ni NPs calculated from the Scherrer equation was 3.48 nm and unit cell di mensions 2.01 Å. The analysis of the Ti(C,N) Ni powders obtained from the synthesis, (not shown), results in a similar pattern that the as received Ti(C,N) powders. Ni is a minor constituent and the estimated amount of Ni in the final composite is close to the detection limit of the equipment, and consequently the overall scan of the composite ma terial only show the Ti(C,N) peaks. However a more accurate scanning

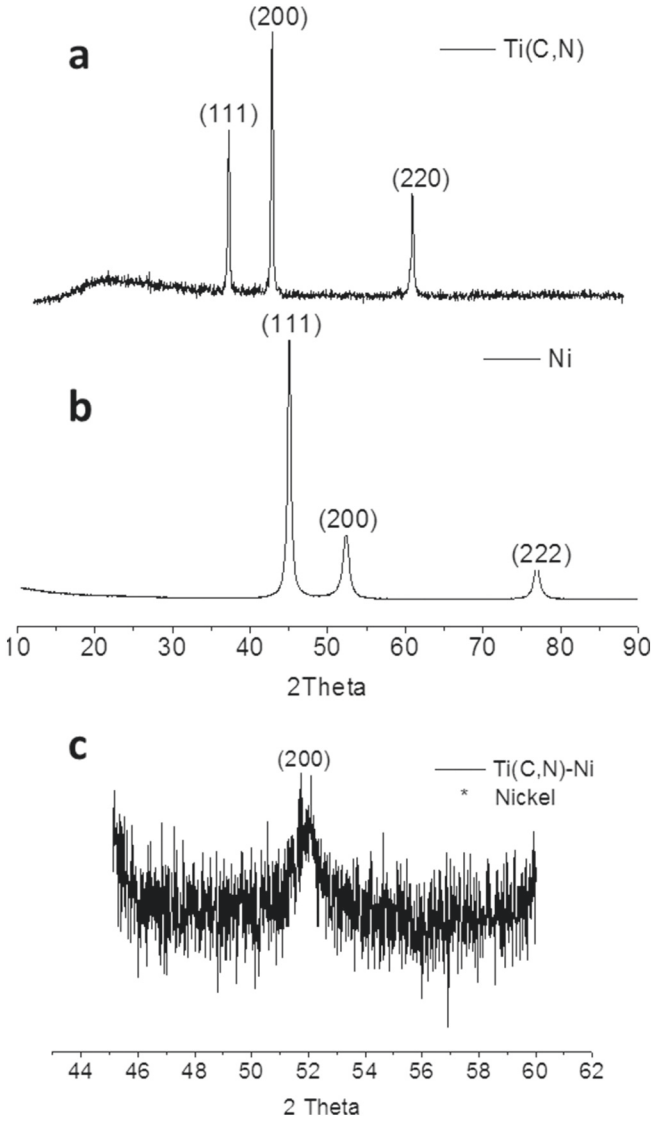

Fig. 1. XRD spectrum of (a) as-received Ti(C,N) particles, (b) Ni NPs and (c) accurate XRD of Ti(C,N)-Ni tailored granules.

(between 45 and 60°) of the composite results in the pattern plotted in Fig. 1c. In this case, the XRD spectrum shows the characteristic peak of FCC Ni lattice (at 52°) which corresponds to the Miller index (200) and that roughly evidences the presence of Ni in the product of the syn thesis. A similar scanning was done for 15 25° to discard the presence of beta $Ni(OH)_2$ ((001) reflection) as residual phase [23].

Previous studies of the morphology and particle size distribution of the as received Ti(C,N) showed that particle population ranges from 200 nm to 2 μm, where a 30% in volume of particles is the fraction of fines ranging 200 300 nm [20]. Fig. 2 shows SEM micrographs of the resulting core shell from the Ni60Hz synthesis in a 3 vol.% suspension of Ti(C,N), (composite 4Ni60Hz), obtained after drying the product of synthesis at room conditions. Although considering the fine fraction of as received Ti(C,N), the exploration of low resolution SEM images of

Table 2
Summary of the formulation of the syntheses and the composition of the produced composites.

Composites	Synthesis	Ni^{2+} concentration	Molar ratio of reactants	Solid content Ti(C,N) suspension	Volumetric ratio of composites
4Ni30Hz	Ni30Hz	0.1 M	1 Ni^{2+}:10 KOH:30 N_2H_4	3 vol.%	96/4 Ti(C,N)/Ni
4Ni60Hz	Ni60Hz	0.1 M	1 Ni^{2+}:10 KOH:60 N_2H_4	3 vol.%	96/4 Ti(C,N)/Ni
10Ni60Hz		0.01 M	1 Ni^{2+}:10 KOH:60 N_2H_4	0.08 vol.%	90/10 Ti(C,N)/Ni

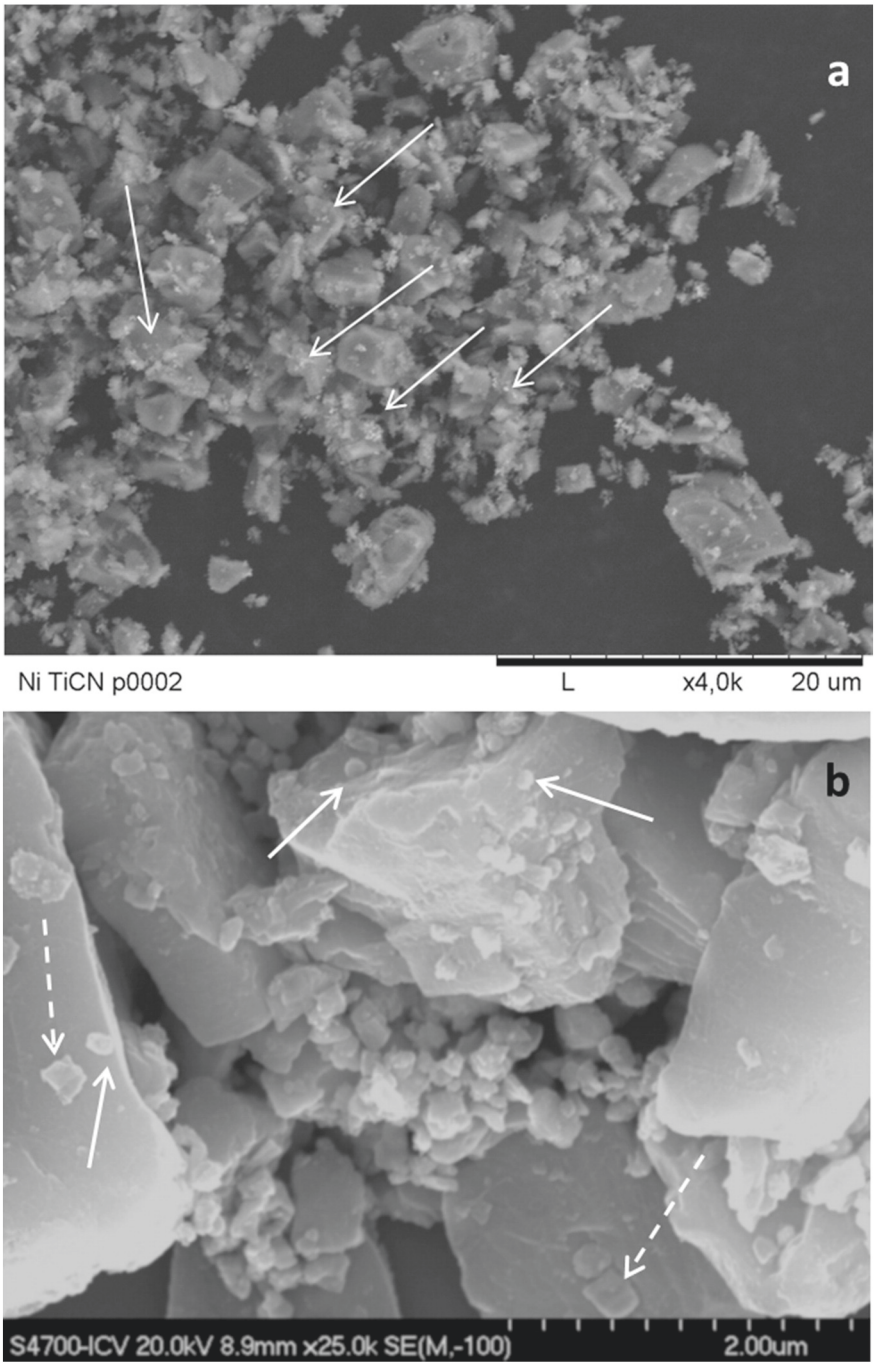

Fig. 2. (a) SEM and (b) FE-SEM micrograph of the Ti(C,N)-Ni core-shell

the composite (Fig. 2a) suggests the presence of sparkling dots ho mogeneously distributed at the sample, which brightness could evi dence the presence of Ni NPs. In Fig. 2b, a high resolution image of the as synthesized composite suggests at least the co existence of two kinds of small particles (100 300 nm) onto the Ti(C,N) coarse faction (particle size > 1 μm). Irregular NPs of 200 nm in size with shaped edges (indicated with dashed arrows) would correspond to the fine fraction of the as received ceramic powder. Whereas that NPs spherical in shape (indicated with straight arrows), slightly smaller with diameters <100 nm, could be assigned to the synthe sized Ni NPs. Elemental analysis of the composition (EDX) of the powders were done and, although the results evidence the presence of Ni, the quantification cannot be identified with the composition of the tailored 4Ni60Hz composite [22].

The study of the morphology, crystallography and composition of the Ti(C,N) Ni powders was completed by HR TEM, STEM, SAED and EDX. Fig. 3 shows a STEM image of 4Ni60Hz composite (a) and the line analysis of the Ni and Ti elements across a Ni Ti(C,N) granule deter mined by EDX (b). The micrograph shows brighter regions around the Ti(C,N) particle corresponding to a continuous layer of Ni which has grown onto the Ti(C,N) surface. As the analysis of the cross section evidences, a Ni layer with a thickness of around 50 nm surrounds the Ti(C,N) particle leading to a composite fashioned in a core shell nanostructure.

Then, the synthesis Ni60Hz was considered to formulate two dif ferent composites, 4Ni60Hz (96/4 v/v Ti(C,N)/Ni) and 10Ni60Hz (90/10 v/v Ti(C,N)/Ni), in order to evaluate the growth behavior of Ni precipitates. Images of both composites obtained after drying at

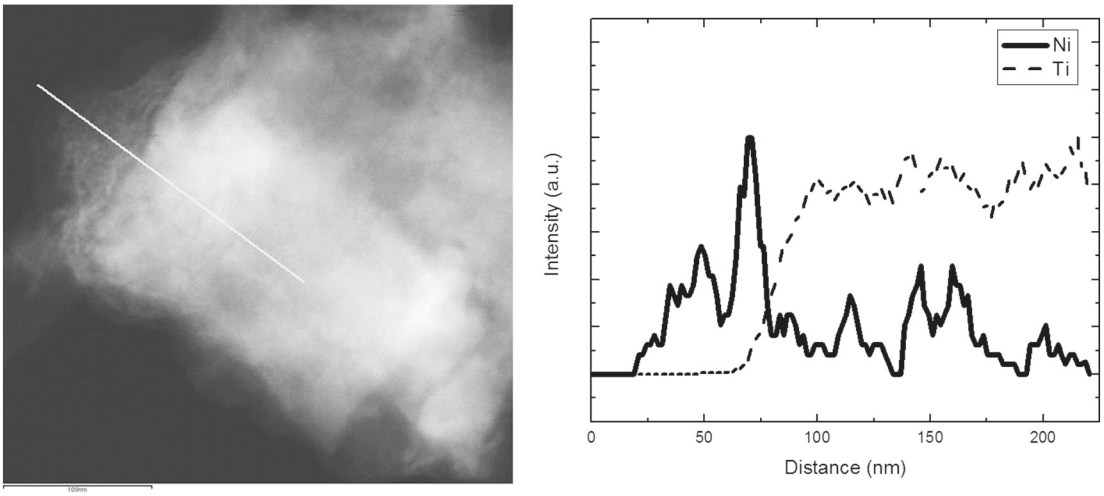

Fig. 3. STEM image of the Ti(C,N) composite (4Ni60Hz) and line profile of the Ni and Ti analysis across the granule

room conditions the resulting powder of synthesis, are showed in Fig. 4. All micrographs evidence the presence of Ni wrapping up the Ti(C,N) particles. For the synthesis performed with a lower con centration of the reactants as well as a lower solid content of Ti(C,N) (10Ni60Hz composite in Table 2), a large amount of Ni NPs are sur rounding the Ti(C,N).

In a general inspection of the product of both syntheses, we can assume that the amount of precipitated Ni decreases with Ti(C,N) coars ening (Fig. 4a, b and d, f). This could be the consequence of the higher specific surface area of the fine fraction of the Ti(C,N) population. Moreover, the formation of flakes or platelets like nanostructures can be appreciated in the HR TEM images in Fig. 4b and c, as a consequence of the polarity of water [16]. Those structures are the precursor feature of the 3D growth of the flower like NPs evidenced in the STEM images in Fig. 4d and e. Flower like NPs fits with the morphology intuited by SEM for the Ni precipitates (Fig. 2a). STEM images of the 4Ni60Hz com posites show in Fig. 4d and e corroborate the massive precipitation of Ni onto the smaller Ti(C,N) particles, either flower shaped or as a layer, surrounding the particle or core ceramic structure (Fig. 4f). Conse quently, the feature of the Ni precipitates changes depending on the

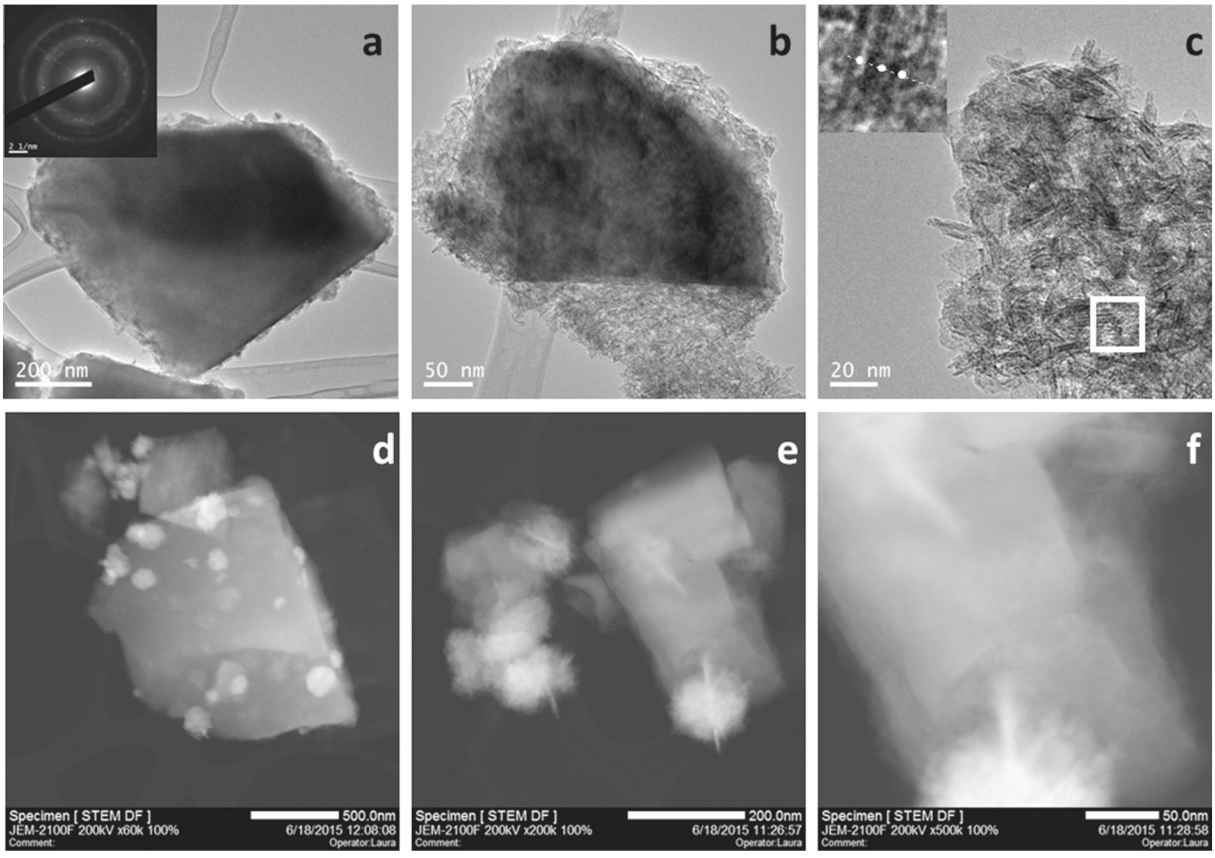

Fig. 4. (a), (b) and (c)HR-TEM micrographs of Ni-Ti(C,N) particles of 10Ni60Hz (d), (e) and (f) STEM micrographs of Ni-Ti(C,N) particles of 4Ni60Hz. Inset (a) show the corresponding nickel SAED pattern.

suspension formulation, basically on the Ni^{2+} concentration [12 17,22] as well as on Ti(C,N) concentration and on the size of the synthesis hold er or surface.

SAED pattern (at the inset of Fig. 4a) reveals that Ni NPs are crystal line or semi crystalline. By measuring the lattice spacing in the HR TEM image (Fig. 4c), the interplanar spacing was found to be 2.0 Å (d spacing ranging 1.95 2.03 Å), corresponding to that between (111) planes of the cubic unit cell, this indicating the formation of pure nickel. This re sult fits those obtained from XRD patterns of Ni NPs obtained in a homo geneous synthesis (Fig. 1b) [22] and those reported for Ni NPs obtained by other synthesis procedures [24].

The Ti(C,N) particles decorated by Ni NPs obtained by chemical re duction and precipitation onto their surface were shaped, following an one pot procedure without employing any drying, separation or wash ing steps. The suspensions obtained after Ni precipitation were directly poured in a mold and shaped by slip casting. After sintering, the micro structure of the obtained bulk pieces was characterized. Fig. 5 shows the SEM micrographs and the EDX analyses of composites 4Ni30Hz and 4Ni60Hz (Table 3), shaped from tailored powders synthesized using dif ferent amounts of hydrazine. Both micrographs show the presence of two phases. The white phase corresponds to the metallic phase, Ni, and the grey phase corresponds to the ceramic phase, Ti(C,N). The in spection of the microstructure evidences the porosity of the bulk piece due to the low solid content of the initial suspension (3 vol.%). In colloi dal processing, solid concentrations lower than 30 vol.% does not use to be considered to process a dense part by slip casting [25]. On the other hand, EDX analyses results are quite diverse depending on the area

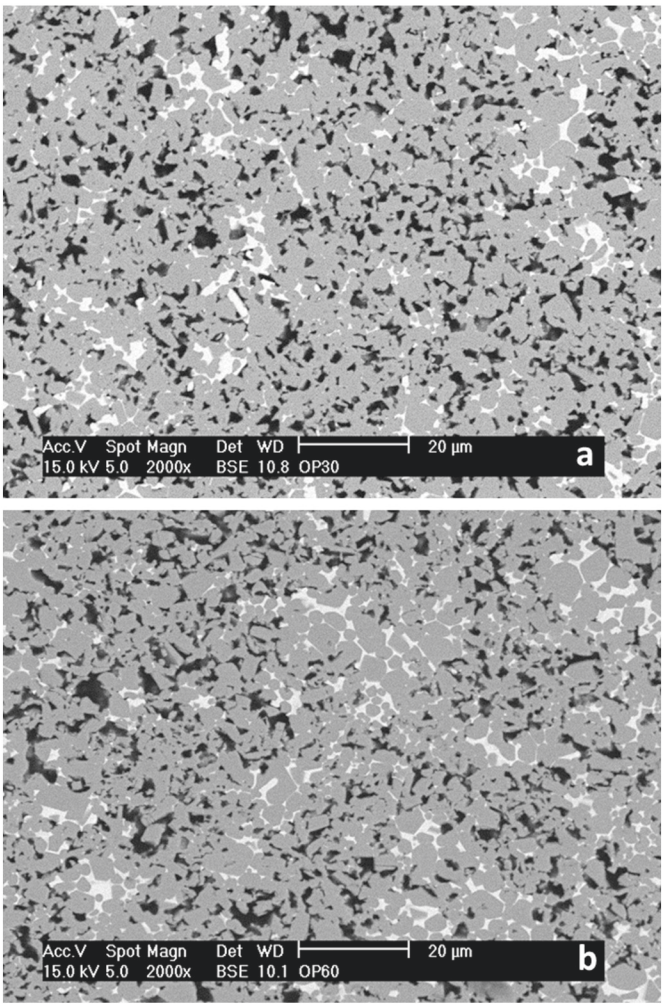

Fig. 5. SEM micrograph of Ti(C,N)-Ni particles (a) 4Ni30Hz and (b) 4Ni60Hz.

Table 3
EDX analysis of Ti(C,N)-Ni particles (a) 4Ni30Hz and (b) 4Ni60Hz.

Material	Compound	wt.% (vol.%)	at.%
4Ni30Hz	Ti(C,N)	86.9 wt.% (91 vol.%)	91.1
	Ni	15.1 wt.% (9 vol.%)	8.9
4Ni60Hz	Ti(C,N)	94.1 wt.% (96.5 vol.%)	93.1
	Ni	5.9 wt.% (3.5 vol.%)	2.9

of the analysis and even on the synthesis conditions (4Ni30Hz or 4Ni60Hz). Results from a wide exploration of each microstructure assign the composition 91/9 v/v to the 4Ni30Hz composite and 96.5/3.5 v/v to the 4Ni60Hz composite. The composition of the samples obtained by the reduction of Ni with a higher amount of hydrazine approaches better the ceramic/metal balance formulated as the starting composition of the composite (see experimental part), which is 96/4 v/v of Ti(C,N) Ni. It evidences the enhanced distribution of the Ni NPs in this microstructure, identifying the optimal conditions of synthesis.

Fig. 6 shows a detail of the microstructure of the 4Ni60Hz composite and the Raman spectra collected at the bulk grain (A) and at the grain boundary (B), as well as that corresponding to a 100% Ti(C,N) sample processed under similar conditions than the composites (C), and used as reference. For sake of comparison, the Raman spectra were collected by using the same laser power (10 mW) and surface Raman images of 50×30 µm. In order to evaluate the effect of Ni content in different areas of our material, we have focused the Raman spectra in a specific region where the vibrational modes of Ti(C,N) appear (from 215 to 300 cm^{-1}). The spectrum corresponding to the as received Ti(C,N) powder is characterized by a monomodal spectrum centered in 270 cm^{-1}, which can be attributed to a Ti(C,N) ternary compound with a high content of C [26]. This peak shifts to lower frequencies in the composite, and a new feature (shoulder) appears in both spectra, at 255 cm^{-1} in that collected at the bulk grain (A) of the microstructure and at 250 cm^{-1} for the spectrum collected at the grain boundary (B). The observed slight position shift of this phonon mode can be attributed to a minor decrease of carbon content in the FCC Ti(C,N) phase in the composite. However, the new shoulder in both spectra evidences differ ent local arrangements due to the presence of Ni in the Ti(C,N) lattice. The effect intensifies at the grain boundary, where the presence of Ni in creases. Consequently, local Raman analyses suggest the solution of the Ni NPs in the Ti(C,N) lattice.

So, despite the density of the final composite, the obtained results al lows us to argue that the sintering process was activated by reducing down to the nanometric size the binder, achieving the Ni solution in the Ti(C,N) lattice. The increment of the surface of reaction with the nanosized metal phase, not only improves the liquid phase distribution among Ti(C,N) particles, but also promote the chemical anchoring with the Ti(C,N) reinforcement phase. Consequently, although the presence of heterogeneities, the microstructure appears well consolidated con trasting with the low amount of Ni (<4 vol.%) in the composite. More over the distribution of the nanometric metal phase leads to a finer microstructure (Fig. 5b), if compare with materials shaped by slip cast ing of high concentrated suspensions of a mixture of micrometric com mercial powders in SS/Ti(C,N) cermets [20]. A complete sintering study to determine the proper sintering conditions for higher density is being conducted; further improvement of the density of the composite will allow to determine the consequences of the potential chemical bond be tween phases as well as the produced finer microstructures resulting from the in situ synthesis of Ni NPs onto Ti(C,N) surfaces.

4. Conclusions

Colloidal processing of Ti(C,N) particles and electroless synthesis of Ni NPs provide a bottom up approach to obtain Ti(C,N)/Ni cermets. The heterogeneous reduction of Ni onto surface of Ti(C,N) particles, de signed for the one pot processing of Ti(C,N)/Ni composites, were

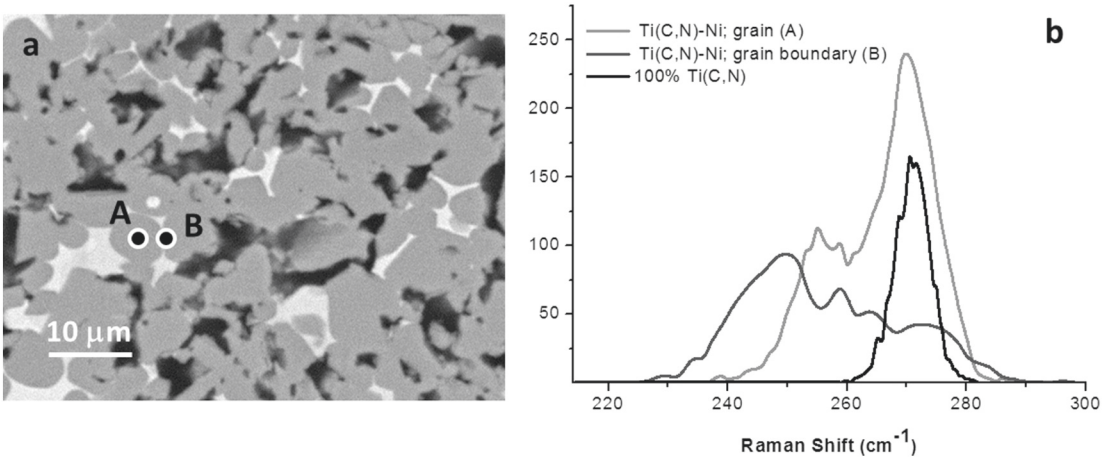

Fig. 6. (a) SEM micrograph of 4Ni60Hz Ti(C,N)-Ni particles and (b) Raman spectra of (A) bulk grain (B) boundary grain and (C) as-received Ti(C,N) particles.

successfully achieved. A very low concentration of metal binder (<4 vol.%) wraps up the ceramic structure leading to a promising micro structure with homogenous and finer distribution of phases, as well as smaller amount of metallic phase.

The optimum conditions of the Ni NPs synthesis include a minimum ratio precursor/hydrazine (~1/60) to provide a homogenous distribu tion of the metal phase in the microstructure. However, the wide size distribution of the micrometric ceramic particles lacks the metal matrix uniformity, because of the fine fraction of powders provides preferential sites for Ni nucleation. Ni NPs precipitate onto Ti(C,N) surfaces taking in flower and flakes like morphologies depending on the solid content of the suspension (amount of Ti(C,N) particles) and the precursor concen tration (amount of Ni^{2+}). Ni nanoplatelets have a diameter of 20 nm and a thickness of 2 4 nm, while flower like particles have 100 nm of diameter. In all cases Ni surrounds Ti(C,N) particles forming a core shell structure.

Acknowledgements

The authors acknowledge the support of the projects S2013/MIT 2862 MAT2015 70780 C4 1 P and MAT2015 70780 C4 2 P. M. De Dios ac knowledges MINECO through the grant BES 2013 065760 and Dr. Z González acknowledges to MINECO through the grant PTQ 13 05985.

Appendix A. Supplementary data

Supplementary data to this article can be found online at http://dx.doi.org/10.1016/j.ijrmhm.2016.08.009.

References

[1] Y. Peng, H. Miao, Z. Peng, Development of TiCN-based cermets: mechanical properties and wear mechanism, RMHM 39 (2013) 78–89, http://dx.doi.org/10.1016/j.ijrmhm.2012.07.001.
[2] D.P. Xiang, Y. Liu, M.J. Tu, Y.Y. Li, W.P. Chen, Synthesis of nano Ti(C,N) powder by mechanical activation and subsequent carbothermal reduction–nitridation reaction, Int. J. Refract. Met. Hard Mater. 27 (2009) 111–114, http://dx.doi.org/10.1016/j.ijrmhm.2008.04.006.
[3] F. Shehata, A. Fathy, M. Abdelhameed, S.F. Moustafa, Fabrication of copper–alumina nanocomposites by mechano-chemical routes, J. Alloys Compd. (2009) http://dx.doi.org/10.1016/j.jallcom.2008.08.065.
[4] J. Sudagar, J. Lian, W. Sha, Electroless nickel, alloy, composite and nano coatings - a critical review, J. Alloys Compd. 571 (2013) 183–204, http://dx.doi.org/10.1016/j.jallcom.2013.03.107.
[5] R.C. Agarwala, V. Agarwala, Electroless alloy/composite coatings: a review, Sadhana 28 (2003) 475–493.
[6] M. Walid, Daoush, Processing and characterization of CNT/Cu nanocomposites by powder technology, Powder Metall. Met. Ceram. 47 (2008) 9–10, http://dx.doi.org/10.1007/s11106-008-9055-x.
[7] M. Uysal, R. Karslio, A. Alp, H. Akbulut, Nanostructured core-shell Ni deposition on SiC particles by alkaline electroless coating, Appl. Surf. Sci. 257 (2011) 10601–10606, http://dx.doi.org/10.1016/j.apsusc.2011.07.057.
[8] H. Zhao, Q. Liang, Y. Lu, Microstructure and properties of copper plating on citric acid modified cotton fabric, Fibers Polym. 16 (2015) 593–598, http://dx.doi.org/10.1007/s12221-015-0593-9.
[9] R.G. Chaudhuri, S. Paria, core/shell nanoparticles: classes, properties, synthesis mechanisms, characterization, and applications, Chem. Rev. 112 (4) (2012) 2373–2433, http://dx.doi.org/10.1021/cr100449n.
[10] S.-H. Wu, D.-H. Chen, Synthesis and characterization of nickel nanoparticles by hydrazine reduction in ethylene glycol, J. Colloid Interface Sci. 259 (2003) 282–286, http://dx.doi.org/10.1016/S0021-9797(02)00135-2.
[11] K.H. Kim, Y.B. Lee, E.Y. Choi, H.C. Park, S.S. Park, Synthesis of nickel powders from various aqueous media through chemical reduction method, Mater. Chem. Phys. 86 (2004) 420–424, http://dx.doi.org/10.1016/j.matchemphys.2004.04.011.
[12] K.H. Kim, Y.B. Lee, S.G. Lee, H. Park, S.S. Park, Preparation of fine nickel powders in aqueous solution under wet chemical process, Mater. Sci. Eng. A 381 (2004) 337–342, http://dx.doi.org/10.1016/j.msea.2004.04.031.
[13] R.-Y. Chen, K.-G. Zhou, Preparation of ultrafine nickel powder by wet chemical process, Trans. Nonferrous Metals Soc. China 16 (2006) 1223–1227, http://dx.doi.org/10.1016/S1003–6326(06)60405–6.
[14] J.W. Park, E.H. Chae, S.H. Kim, J.H. Lee, J.W. Kim, S.M. Yoon, et al., Preparation of fine Ni powders from nickel hydrazine complex, Mater. Chem. Phys. 97 (2006) 371–378, http://dx.doi.org/10.1016/j.matchemphys.2005.08.028.
[15] G.G. Couto, J.J. Klein, W.H. Schreiner, D.H. Mosca, A.J. de Oliveira, A.J. Zarbin, Nickel nanoparticles obtained by a modified polyol process: synthesis, characterization, and magnetic properties, J. Colloid Interface Sci. 311 (2007) 461–468, http://dx.doi.org/10.1016/j.jcis.2007.03.045.
[16] D.-P. Wang, D.-B. Sun, H.-Y. Yu, H.-M. Meng, Morphology controllable synthesis of nickel nanopowders by chemical reduction process, J. Cryst. Growth 310 (2008) 1195–1201, http://dx.doi.org/10.1016/j.jcrysgro.2007.12.052.
[17] Z.G. Wu, M. Munoz, O. Montero, The synthesis of nickel nanoparticles by hydrazine reduction, Adv. Powder Technol. 21 (2010) 165–168, http://dx.doi.org/10.1016/j.apt.2009.10.012.
[18] J. Tientong, S. Garcia, C.R. Thurber, T.D. Golden, Synthesis of nickel and nickel hydroxide nanopowders by simplified chemical reduction, J. Nanotechnol. (2014) http://dx.doi.org/10.1155/2014/193162.
[19] M. Dios, Z. Gonzalez, E. Gordo, B. Ferrari, Semiconductor-metal Core-shell Nanostructures by Colloidal Heterocoagulation in Aqueous Medium, 2016 (doi: 10.1016/j.matlet.2016.05.179).
[20] J.A. Escribano, J.L. García, P. Alvaredo, B. Ferrari, E. Gordo, A.J. Sanchez-Herencia, FGM stainless steel-Ti(C,N) cermets through colloidal processing, Int. J. Refract. Met. Hard Mater. 49 (2014) 143–152, http://dx.doi.org/10.1016/j.ijrmhm.2014.05.008.
[21] P. Alvaredo, S.A. Tsipas, E. Gordo, Influence of carbon content on the sinterability of an FeCr matrix cermet reinforced with TiCN, RMHM 36 (2013) 283–288, http://dx.doi.org/10.1016/j.ijrmhm.2012.10.007.
[22] M. Dios, Z. González, E. Gordo, B. Ferrari, Core-shell Ti(C,N)-Ni structures fabricated by chemical precipitation of Ni-based nanoparticles on Ti(C,N) suspensions EURO PM 2015, Proceeding EURO PM 2015, 2015.
[23] A. Caballero, L. Hernán, J. Morales, S. Cabanas-Polo, B. Ferrari, A.J. Sanchez-Herencia, et al., Electrochemical properties of ultrasonically prepared $Ni(OH)_2$ nanosheets in lithium cells, J. Power Sources 238 (2013) 366–371, http://dx.doi.org/10.1016/j.jpowsour.2013.04.033.
[24] Y. He, X. Li, M.T. Swihart, Laser-driven aerosol synthesis of nickel nanoparticles, Chem. Mater. 17 (2005) 1017–1026, http://dx.doi.org/10.1021/cm048128t.
[25] N. Hernández, A.J. Sánchez-Herencia, R. Moreno, Forming of nickel compacts by a colloidal filtration route, Acta Mater. 53 (2005) 919–925, http://dx.doi.org/10.1016/j.actamat.2004.10.038.
[26] L. Escobar-Alarcon, E. Camps, S. Romero, S. Muhl, I. Camps, E. Haro-Poniatowski, TiCN thin films grown by reactive crossed beam pulsed laser deposition, Appl. Phys. A Mater. Sci. Process. (2010) http://dx.doi.org/10.1007/s00339-010-5935-2.